On the existence and stability of bulk nanobubbles

Nirmalkar, Neelkanth; Pacek, Andrzej; Barigou, Mostafa

[Link to publication on Research at Birmingham portal](#)

LANGMUIR

Article

pubs.acs.org/Langmuir

On the Existence and Stability of Bulk Nanobubbles

N. Nirmalkar, A. W. Pacek, and M. Barigou*

School of Chemical Engineering, University of Birmingham, Edgbaston, Birmingham B15 2TT, U.K.

S Supporting Information

ABSTRACT: Bulk nanobubbles are a novel type of nanoscale bubble system. Because of their extraordinary behavior, however, their existence is not widely accepted. In this paper, we shed light on the hypothesis that bulk nanobubbles do exist, they are filled with gas, and they survive for long periods of time, challenging present theories. An acoustic cavitation technique has been used to produce bulk nanobubbles in pure water in relatively large numbers approaching 10^9 bubble·mL^{-1} with a typical diameter of 100−120 nm. We provide multiple evidence that the nanoentities observed in suspension are nanobubbles given that they disappear after freezing and thawing of the suspensions, their nucleation rate depends strongly on the amount of air dissolved in water, and they gradually disappear over time. The bulk nanobubble suspensions were stable over periods of many months during which time the mean diameter remained unchanged, suggesting the absence of significant bubble coalescence, bubble breakage, or Ostwald ripening effects. Measurements suggest that these nanobubbles are negatively charged and their zeta potential does not vary over time. The presence of such a constant charge on the nanobubble surfaces is probably responsible for their stability. The effects of pH, salt, and surfactant addition on their colloidal stability are similar to those reported in the literature for solid nanoparticle suspensions, that is, nanobubbles are more stable in an alkaline medium than in an acidic one; the addition of salt to a nanobubble suspension drives the negative zeta potential toward zero, thus reducing the repulsive electrostatic forces between nanobubbles; and the addition of an anionic surfactant increases the magnitude of the negative zeta potential, thus improving nanobubble electrostatic stabilization.
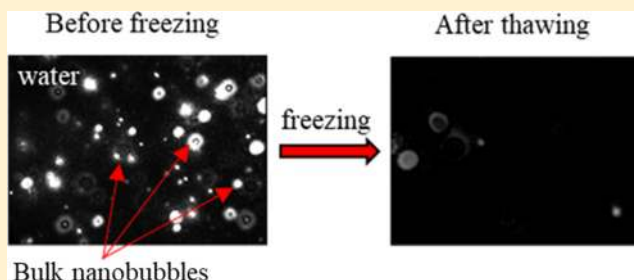
INTRODUCTION

In recent years, three new types of nanoscale bubble systems have been reported: (i) surface nanobubbles which form at solid−liquid interfaces and are either (i) spherical cap bubbles or (ii) micropancakes which are quasi-two-dimensional gaseous domains, with lateral dimensions of several microns and a uniform height of a few nanometers; and much more recently (iii) bulk nanobubbles which exist in bulk liquid and are spherical with a typical diameter of 100−200 nm. The most peculiar characteristic of these three types of nanobubbles is their extraordinary longevity.[1] Because of established bubble theories, early reports on stable nanobubbles at surfaces were met with scepticism and an accepted description of their stability is still lacking. Surface nanobubbles were until recently a controversial topic despite mounting evidence for their existence which is now firmly established, following investigations by a number of research groups.[1] Similarly, despite a number of recent studies,[2] bulk nanobubbles are still an emerging field and speculation remains rife about their existence and their stability.[3,4]

In pure water, the pressure estimated from the Young−Laplace equation inside a nanobubble of 100 nm diameter is close to ~30 atm; therefore, from the Epstein and Plesset[5] theory, the bubble should dissolve on a timescale of ~10 μs. However, bulk nanobubbles have been reported to last for days, weeks, and months.[1,2,6] There are two aspects associated with the long-term stability of bulk nanobubbles. The first one is the negligible buoyant force which prevents bulk nanobubbles from rising to the free surface, their movement being instead dominated by Brownian motion. The second is their stability against dissolution. The physical chemistry of this longevity is an observational mystery that is now attracting considerable attention.[2]

The mystery behind the stability of bulk nanobubbles has led some to consider them as heterogeneities which are preserved, similar to imperfections in a crystalline structure.[7] Some investigators reported that degassing or repeated filtering can remove them and that subsequent gentle gas sparging can restore them, which seems to suggest that the nucleation centers must remain in the bulk liquid.[4] Others have speculated that interfacial composition and structure are the likely cause for nanobubble stability, with some suggesting that the surface of nanobubbles contains hard hydrogen bonds which may reduce gas diffusivity.[2] Another speculation considers that a trapped layer of insoluble contaminant coats each nanobubble reducing the interfacial tension (and Laplace pressure) and imposing a barrier to diffusion.[8] The idea of "universal" contamination is questionable however because thermal fluctuations are bound to create pores in the contaminant shell and thus lead to gas escaping with time.

Even more convincing perhaps is the fact that our own tests revealed that in normal distilled water or even tap water, nanobubbles would be observed only if they have been generated by some external means. Recently, a theoretical dynamic equilibrium model hypothesized that bulk nanobubbles could be partly covered by a hydrophobic material.[9] The dynamic equilibrium model assumes a continuous inflow and outflow of gas from the nanobubbles which maintain their size constant. On the basis of the assumptions that the total change in entropy and energy is both zero in a state of equilibrium, it is found numerically that nanobubbles are stable when the surface coverage fraction lies within 0.5−1. More recently, Sugano et al.[10] reported an experimental study where they used transmission electron microscopy (TEM) images of bulk nanobubbles taken by using a MEMS chip without freezing, to show that added organic material adhered to the surface of nanobubbles which contributed to their stability.

Bulk nanobubbles are recent but they are already attracting a lot of attention, and many potential applications have been suggested including, wastewater treatment,[11] surface cleaning,[12−14] froth flotation,[15−19] nanobubbles as an ultrasound (US) contrast agent,[20−25] therapeutic drug delivery,[24−27] drag reduction,[28] promotion of the physiological activity of living organisms,[6] sterilization of bacteria,[29] enhanced germination rate of seeds,[30,31] improved blood oxygenation,[32] and improved engine efficacy using hydrogen nanobubbles.[33,34] There is, thus, immense scope for bulk nanobubbles to impact many industries. To fully exploit these potential benefits, however, a thorough understanding of their formation, characterization, and stability is needed.

In this paper, we study the generation of bulk nanobubbles in water using acoustic cavitation. For the first time, we provide multiple evidence that the nanoentities generated are nanobubbles based on: (i) freezing and thawing of the nanobubble suspensions; (ii) the relationship between the amount of dissolved air and the number of bulk nanobubbles generated in water; and (iii) monitoring of their gradual disappearance over time. We also study the effects of water pH as well as surfactant and salt addition on the stability of the nanobubbles. The long-term stability of the bulk nanobubble suspensions is monitored over a period of 10 months. We conclude that bulk nanobubbles carry a significant surface charge which is probably responsible for their stability.

■ EXPERIMENTAL METHODS

Materials. Sodium chloride (NaCl, 99.5% BioXtra), sodium dodecyl sulfate (SDS, AR > 99%), and buffer solutions (pH = 4, 7, and 10) were purchased from Sigma-Aldrich. Sodium hydroxide (NaOH, 98%) and hydrochloric acid (HCl, 37%) were purchased from VMR Chemicals. All stock solutions and nanobubble samples were prepared using purified water from an Aquatron water still A4000D, which had an electrical conductivity of 1.7 μS·cm^{-1} and a pH of 6.5. This water is referred to as pure water throughout the paper to distinguish it from water with added salt or surfactant. Stock solutions of SDS were prepared by dissolving SDS in pure water using a magnetic stirrer at 25 °C in order to achieve complete dissolution. A 0.45 μm Millipore filter (Merck Millipore Limited, UK) was used to filter the SDS solutions. A similar protocol was adopted for preparing stock solutions of NaOH, HCl, and NaCl at a temperature of 20 °C. Prior to experimentation, purified water and all stock solutions were initially examined for any nanoscale entities using a NanoSight instrument and no significant levels of impurity were observed. The NanoSight instrument which was also used for measuring nanobubble size distributions is described further below.

Generation of Bulk Nanobubbles. Nanobubbles were generated by US cavitation using a 20 kHz probe-type US processor (AUTOTUNE SERIES 750 W model, Sonics & Materials). A titanium probe of 0.75 in. diameter was used to irradiate 80 mL of water inside a glass beaker, as shown in Figure 1. The temperature of
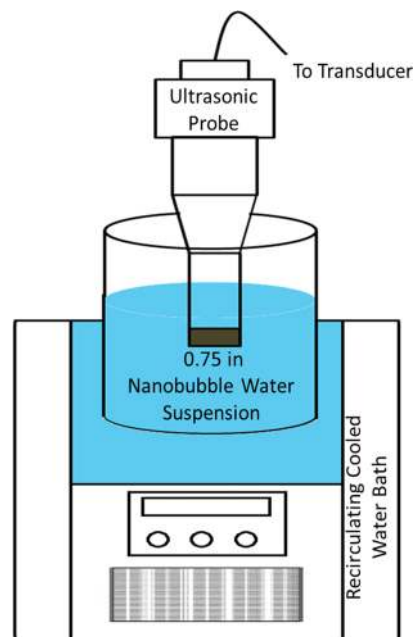
Figure 1. Schematics of experimental rig.

the sample was controlled at 20.0 °C by using a recirculating cooler (JULABO GmbH, Germany). The sonication time and, hence, the US energy input were varied in the experiments, and the effects were investigated. After sonication, the nanobubble suspension, thus generated, was stored in 20 mL glass vials for further analysis of bubble size distribution, bubble number density, zeta potential, dissolved oxygen content, and monitoring of long-term stability. All analyses of the nanobubble samples were conducted at room temperature.

Characterization of Bulk Nanobubble Suspensions. *Nanoparticle Tracking Analysis.* Bubble size distribution was characterized using a NanoSight LM10 instrument (Malvern Instruments, UK). The NanoSight technique called nanoparticle tracking analysis (NTA) is a noninvasive technique and is schematically illustrated in Figure S1a in the Supporting Information. It utilizes the properties of both light scattering and Brownian motion in order to obtain particle size distributions of samples in liquid suspension. A laser beam is passed through a prism-edged glass flat (optical flat) within the sample chamber. The angle of incidence and refractive index of the glass flat are designed to be such that when the laser reaches the interface between the glass and the liquid sample layer above it, the beam refracts to an intense low profile resulting in a compressed beam with a reduced profile and a high-power density. Particles in the path of this beam scatter light and can be easily visualized via a long working distance (×20 magnification) microscope objective fitted to an otherwise conventional optical microscope. A charge-coupled device (CCD), electron multiplied CCD, or high-sensitivity CMOS camera mounted on the microscope and operating at 30 frames per second captures a video file of particles moving under Brownian motion. Nanoparticles or nanobubbles are, thus, indirectly tracked, and their Brownian motion is analyzed in real time, giving the bubble size distribution, mean bubble diameter, and bubble number density.

Brownian motion occurs in three dimensions, but the NTA instrument observes motion only in two dimensions. The 2D tracking of nanobubbles can be utilized to calculate the diffusion coefficient of Brownian motion using the following form of the well-known Einstein−Stokes equation, as follows[35]

$$\frac{\overline{(x, y)^2}}{4t} = D_t = \frac{k_B T}{3\pi\mu d} \tag{1}$$

where $\overline{(x, y)^2}$ is the mean square displacement of a nanoparticle in two dimensions measured in time t. The parameters D_t, k_B, T, μ, and d are, respectively, diffusion coefficient, Boltzmann constant, temperature, viscosity, and diameter of the particle. Because of the fact that this technique can simultaneously analyze a population of nanoparticles on an individual basis, it is ideally suited for real-time analysis of polydisperse systems ranging from 10 to 2000 nm in size and 10^6 to 10^9 particles/mL in particle number density.[36]

Dynamic Light Scattering. A dynamic light scattering (DLS) technique (ZEN5600 Zetasizer Nano ZSP, Malvern Instruments) was also used to determine the bubble size distribution of the nanobubble suspensions. The objective was to compare the bubble size distributions obtained from DLS with those obtained from NTA measurements and assess the suitability of the two techniques for characterizing nanobubble suspensions. DLS is a well-established noninvasive technique for measuring the size distribution of particles typically in the submicron region. Typical applications of DLS are the characterization of particles, emulsions, or molecules which have been dispersed or dissolved in a liquid. The Brownian motion of particles or molecules in suspension causes laser light to be scattered at different intensities, as illustrated in Figure S1b in the Supporting Information. Analysis of these intensity fluctuations yields the velocity of the Brownian motion and hence the particle size using the Einstein−Stokes relationship (eq 1).[37] DLS is suitable for particle analysis over a size and concentration range of 0.3 nm to 10 μm and 10^8 to 10^{12} particles/mL, respectively.[38,39] DLS, however, does not measure the bubble number density. Prior to analysis of the nanobubble samples, standard suspensions of solid latex nanospheres were used to verify the accuracy and precision of the NTA and DLS systems used and adjust the settings of the instruments accordingly.

Zeta Potential, pH, and Dissolved Oxygen Content. The Zetasizer Nano ZSP described above also enabled the measurement of the zeta potential of the nanobubbles. Similarly, a pH meter (Mettler Toledo) was calibrated using standard buffer solutions and used to measure the pH of the nanobubble suspensions. Furthermore, the pH of the nanobubble samples was adjusted by drop wise addition of NaOH or HCl, covering a wide range of pH values. A dissolved oxygen meter (model AM 40, Sensortechnik Meinsberg, Germany) was used to determine the dissolved oxygen concentration in the nanobubble suspensions.

Bubble Size Distribution Measurement Using NTA and DLS Techniques. A comparison was made between the NTA and DLS techniques to assess which is the more appropriate technique for the analysis of bulk nanobubble suspensions. Typical bubble size distributions determined by both methods are compared in Figure S2 of the Supporting Information, showing significant differences. There is a clear shift in the bubble size distribution measured by NTA toward the lower end of the bubble size spectrum (number mean diameter, d_{10} = 137 nm compared to 173 nm obtained by DLS). This is accompanied by a significant narrowing of the bubble size distribution obtained by NTA: C_v values are 0.58 for NTA and 1.73 for DLS, kurtosis values are −1.2 for NTA (positively skewed, leptokurtic distribution) and 4.43 for DLS (positively skewed, platykurtic distribution).

As DLS is based on the intensity of scattered light, larger bubbles will scatter more light and, hence, will tend to mask light scattered by smaller bubbles. A similar result was reported by Filipe et al.[39] who compared the size distributions of standard latex nanoparticle suspensions determined by NTA and DLS. The fact that NTA tracks the Brownian motion of nanobubbles should make it a more reliable technique compared to DLS whose measurements are based on the intensity of scattered light and clearly, thus, are biased toward large bubbles. Hence, the NTA technique has been adopted in this study for the characterization of the nanobubble suspensions.

■ RESULTS AND DISCUSSION

Existence of Bulk Nanobubbles. As discussed in the Introduction, the existence of bulk nanobubbles has been claimed in several recent experimental studies but definite proof that the nanoentities observed are actually gas bubbles is still missing.[2,11,13,40] Despite such studies, therefore, this is still an emerging field and speculation remains rife about the existence of bulk nanobubbles and their stability.[41] In mixtures of water and organic liquids, doubt exists as to whether the nanoentities observed are nanobubbles or supramolecular structures.[3,4] Similarly, when generating bulk nanobubbles in pure water, another question that often arises is whether such nanoentities are nanobubbles or solid nanoparticles which have detached from adjacent surfaces.

In this work, we provide evidence for the existence of bulk nanobubbles in three different ways: (i) by studying the effect of freezing and thawing on nanobubble suspensions in pure water and in the presence of added surfactant; (ii) by analyzing the effect of dissolved gas on the nucleation of nanobubbles; and (iii) by monitoring the long-term stability of bulk nanobubbles and their gradual disappearance over time.

Freezing and Thawing of Nanobubbles in Pure Water and in Surfactant Solution. Experiments were conducted to study what happens when bulk nanobubble suspensions are subjected to freezing and thawing. Thus, 20 mL samples of nanobubble suspensions produced in pure water were kept in a freezer at a temperature of −18 °C for a period of 24 h. Subsequently, these samples were withdrawn from the freezer and left to thaw at room temperature for about 6 h before being analyzed by the NTA technique. Typical results of the effects of the freeze−thaw process on the bubble number density and bubble size distribution are shown in Figures 2 and 3, respectively.
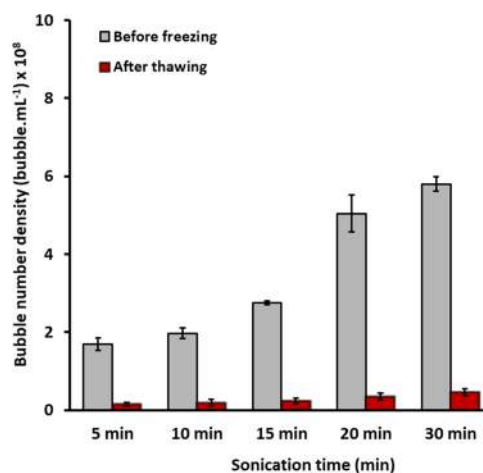
Figure 2. Freezing and thawing of bulk nanobubble suspensions generated in pure water at different sonication times.

On increasing the sonication time (i.e., US energy input), the population of the nanobubbles produced increased substantially. After freezing and thawing of the nanobubble suspensions, the bubble number density reduced to extremely low levels approaching zero at low sonication times. It is hard to tell whether nanobubble disappearance occurs during freezing or thawing. Given that the freezing rate is very low, one could imagine that nanobubbles will be pressed to move and coalesce or agglomerate by the growing ice crystals in a
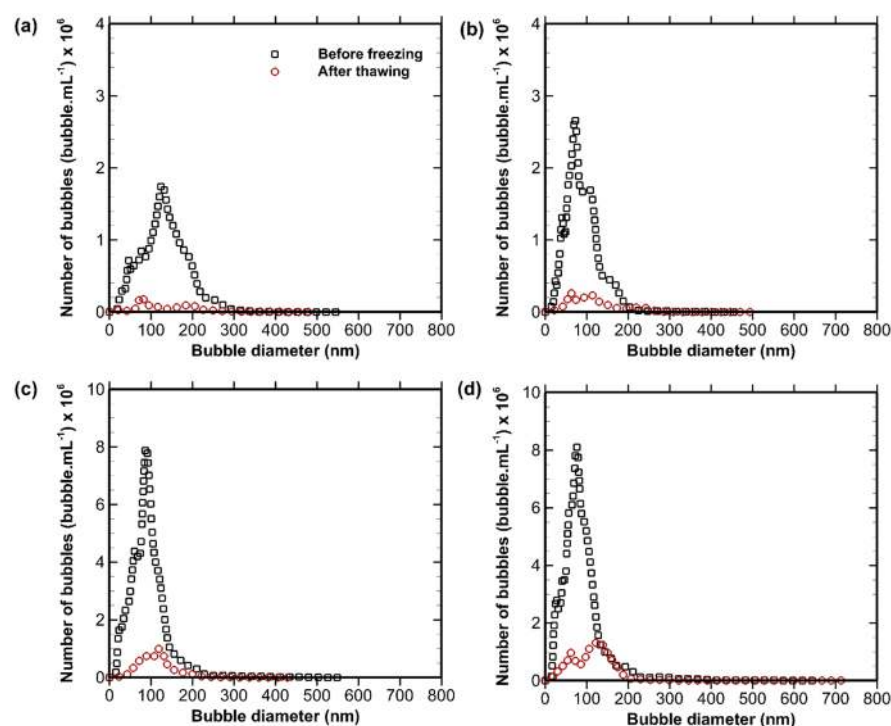
Figure 3. Bubble size distributions before freezing and after thawing of nanobubble suspensions generated in pure water at different sonication times: (a) 5; (b) 10; (c) 20; and (d) 30 min.

way similar to the process of freeze concentration, leading eventually to rupture of the nanobubble interfaces. However, it is much harder to speculate on a possible mechanism for nanobubble disappearance during thawing.

The size distributions shown in Figure 3 confirm that the large reduction in the number of nanoentities cannot be explained by the possibility of agglomeration of nanoparticles. No significant aggregation could have happened because the statistics of the size distribution before freezing and after thawing remain approximately the same. Had any significant aggregation happened the size distribution would have exhibited a large positive skew. The fact that the vast majority of the nanoentities disappeared during freezing and thawing of the samples implies that these must be bubbles.

On the other hand, more freeze−thaw cycles did not lead to any further significant reductions in the number of residual nanoentities observed. The small amount of residual nano-entities which have not disappeared, therefore, must be solid nanoparticles. This amount of nanoparticles is negligible at low-energy inputs as it increases from 4.5% at a sonication time of 5 min to a maximum of 9.2% at a sonication time of 30 min. In addition to a low level of initial contamination contained in the purified water, these solid nanoparticles could be titanium nanoparticles which have detached during sonication from the US probe or particles which have detached from the surfaces of the glass beaker, which could also explain why their number increases with sonication time. However, in routine experi-ments, the sonication time normally used was 10 min maximum, which does not lead to any significant contami-nation of the samples.

Similar experiments were conducted whereby different amounts of the surface-active agent SDS were added to the nanobubble suspensions produced in pure water before freezing, and the results are shown in Figure 4. Whilst nanobubbles in pure water disappear after freezing and
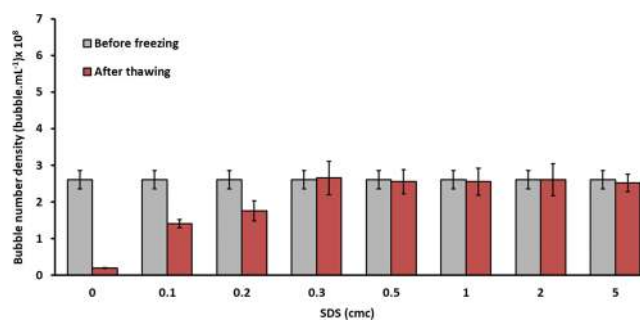

Figure 4. Freezing and thawing of bulk nanobubble suspensions produced in pure water and having different amounts of SDS surfactant added (sonication time was 10 min, equivalent to ∼35 kJ of US energy input).

thawing, the presence of SDS seems to prevent the collapse of nanobubbles and for concentrations of 0.3 cmc (critical micelle concentration) and above, the nanobubble population is entirely preserved within experimental error. It should be noted that the observed effect cannot be attributed to the presence of SDS micelles as they are too small to be detected by the NTA measurements. Their radius in aqueous solutions is only about 1.75 nm[42] which is much below the resolution of the instrument. Therefore, it can be concluded from these experiments that surfactant molecules provide shielding to the nanobubbles against the effects of freezing and thawing, a phenomenon widely known in colloidal science as steric/electro-steric stabilization of particle suspensions.[43]

The survival of bulk nanobubbles through the freeze−thaw process can be further explained by the mechanism of stabilization of nanoparticles with the addition of surfactants. In pure water, our zeta potential measurements show that nanobubbles are negatively charged. On the nanobubble interfaces, the hydrophilic ionic head group SO_4^- of the SDS

molecules orientates itself toward the liquid phase whilst the hydrophobic tail orientates itself toward the gas phase. This preferential adsorption of the surfactant molecules is expected to reduce surface tension and, hence, the Laplace pressure inside the nanobubbles, which further their stability. Recent use of pressure-addition electrochemistry[44] showed that Laplace pressure decreases by ∼42% in the presence of surfactant where the corresponding macroscopic surface tension drops by 45% from 73 to 33 mN·m^{-1} for an 88 nm radius nanobubble. This result seems to apparently confirm the validity of the Young−Laplace equation at nanoscale and also provide experimental evidence of the reduction of Laplace pressure in the presence of surfactant molecules. Incidentally, the findings from the above freeze−thaw experiments clearly rule out the validity of the skin physical model which postulates that bulk nanobubbles are stable because of the presence of organic contaminants or surfactant molecules on the surface of the nanobubbles which provide stability against dissolution.[7,45]

Dissolved Oxygen Content in Nanobubble Suspensions. Measurements (conducted at 20 °C) of dissolved oxygen concentration in the nanobubble samples are presented in Figure 5 and compared to pure water. The amount of
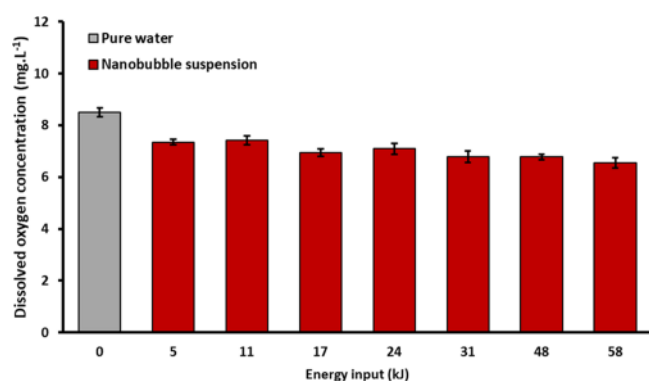
Figure 5. Dissolved oxygen content in nanobubble suspensions generated at different US energy inputs.

dissolved oxygen in pure water drops significantly, on average by about 20%, after the generation of nanobubbles. It is expected that dissolved gas molecules act as nuclei for US cavitation. In fact, increased content of dissolved gases in water has been shown to improve acoustic cavitation intensity for the generation of microbubbles and their growth rate.[46] Our results also suggest that dissolved gas has a positive correlation with the nucleation of nanobubbles. Experiments were conducted by generating nanobubbles in pure water which was partially degassed using vacuum, and typical results are shown in Figure 6. The data show that the higher the oxygen concentration in water, the more bubbles are generated. This finding indicates, therefore, that dissolved gas seems to be needed for the generation of these nanoentities which by implication suggests that they must be nanobubbles. It should be noted that these findings are specific to the case of acoustic cavitation where no additional air is injected unlike, for example, hydrodynamic cavitation (pressure dissolution method).[11]

Effect of Water pH on Nanobubble Nucleation. In this section, we study the effects of preadjusting the water pH on the properties of the bulk nanobubble suspensions subsequently generated by US cavitation. Results are displayed
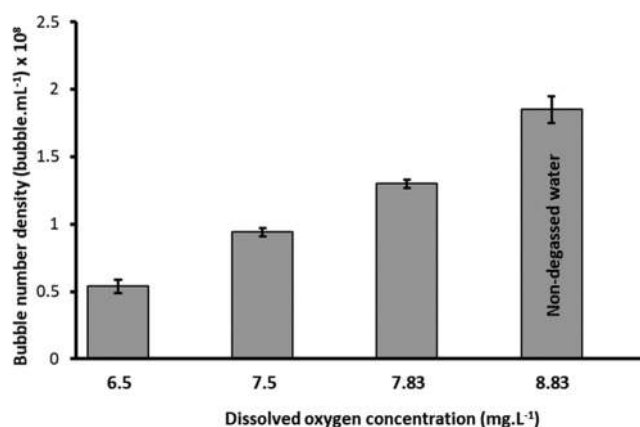
Figure 6. Effect of dissolved air content on nucleation of bulk nanobubbles (sonication time was 5 min, equivalent to 18 kJ US energy input).

in Figure 7 in terms of bubble size distribution, mean bubble diameter, bubble number density, and zeta potential. The number density of nanobubbles increases in a quasi-linear fashion as a function of pH. The mean bubble diameter decreases as the water pH increases to a value of about 6, remaining more or less constant thereafter at higher pH values. The zeta potential is negative and increases in absolute value with increasing pH approximately linearly, reaching substantial magnitudes (around −40 mV) at high pH values (Figure 7d). A high zeta potential is synonymous with high colloidal stability which suggests that nanobubbles should be much more stable in alkaline solutions. This result can be explained based on the fact that nanobubbles can nucleate at all values of water pH as long as there is sufficient dissolved gas to provide the necessary nuclei. However, many of the nanobubbles cannot survive at low pH values because of a lack of OH$^-$ ions needed to form a stabilizing electric double layer around the bubble interfaces, as indicated by the low values of zeta potential (Figure 7d). The high zeta potential in alkaline solutions is evidence of strong electrostatic interaction providing stability to the system and, thus, alkaline solutions are a more favorable medium for the formation and stability of nanobubbles than acidic solutions.

Zeta Potential of Nanobubbles. The colloidal stability of a particle suspension depends on Derjaguin−Landau−Verwey−Overbeek (DLVO) and non-DLVO forces, namely, van der Waals forces, electrostatic forces, hydration forces, hydrophobic interaction, and steric forces. The overall interaction potential for a suspension is usually denoted by the algebraic sum of DLVO and non-DLVO interactions, and the suspension stability depends on the interplay between these interactions.[43] The electric double layer around the particles can be altered by the addition of salt or adjustment of pH, whilst the addition of surfactant leads to steric stability of the particles. To shed light on some of these phenomena, we propose here to look at the effects of pH adjustment, salt, or surfactant addition on the zeta potential of bulk nanobubbles, note that the nanobubble suspensions were first produced in pure water and then subsequently altered.

Results showing the effects on zeta potential are presented in Figure 8. The magnitude of the negative zeta potential increases monotonically as a function of pH in a quasi-linear fashion (Figure 8a). This is consistent with the usual behavior of colloidal particle suspensions.[43] Because the slipping plane is
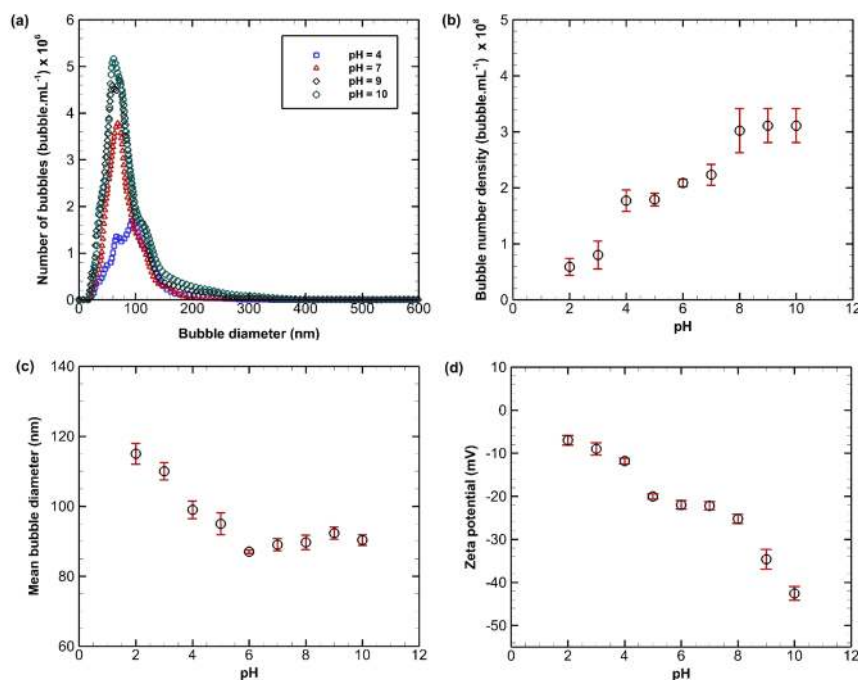
Figure 7. Effects of preadjustment of water pH on US-generated bulk nanobubble suspensions.
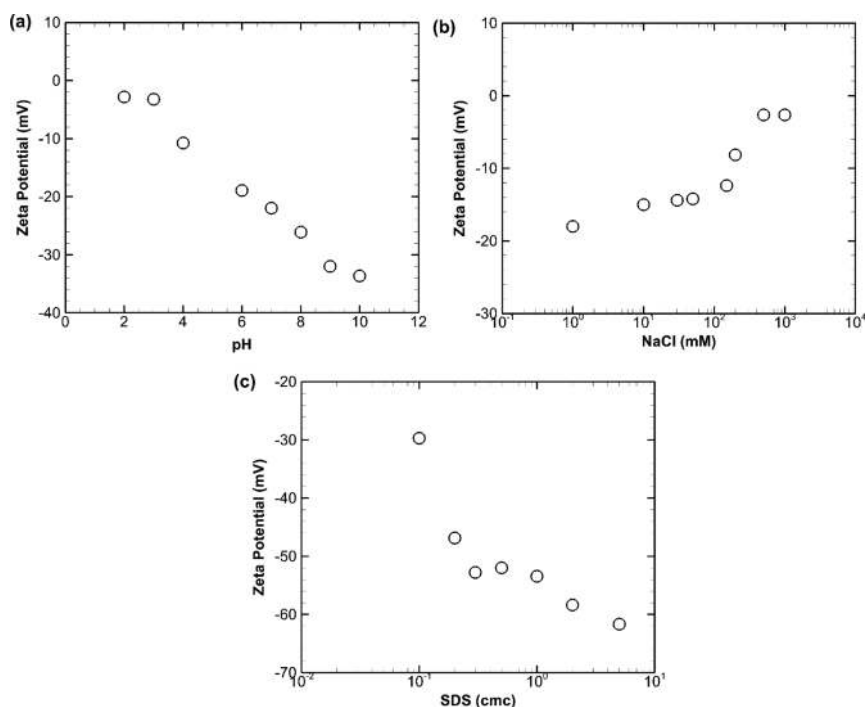
Figure 8. Zeta potential of bulk nanobubbles: (a) effect of pH adjustment; (b) effect of added NaCl salt concentration; and (c) effect of added anionic SDS surfactant concentration.

negatively charged at pH = 7, the addition of H$^+$ ions (from HCl) to lower the pH value neutralizes the negative charge. This reduces the absolute value of the negative zeta potential toward zero, and hence, it weakens the electrostatic interaction potential between nanobubbles as expressed below[43]

$$W_R(D) = \frac{64 k_B T R \rho_\infty}{\kappa^2} \tan h^2 \left(\frac{z e \psi_0}{4 k_B T} \right) \exp(-\kappa D) \qquad (2)$$

where $W_R(D)$, R, k_B, T, z, ψ_0, e, ρ_∞, and D are, respectively, electrostatic potential, bubble radius, Boltzmann constant, temperature, valency, surface potential, unit charge, bulk ion number density, and interspacing distance. On the other hand, the magnitude of the negative zeta potential of the nanobubbles increases in alkaline solutions reaching a value of about −32 mV at pH = 10. We, therefore, reach the same conclusion as before when the water pH was preadjusted before the generation of the nanobubbles (Figure 7d), that is,
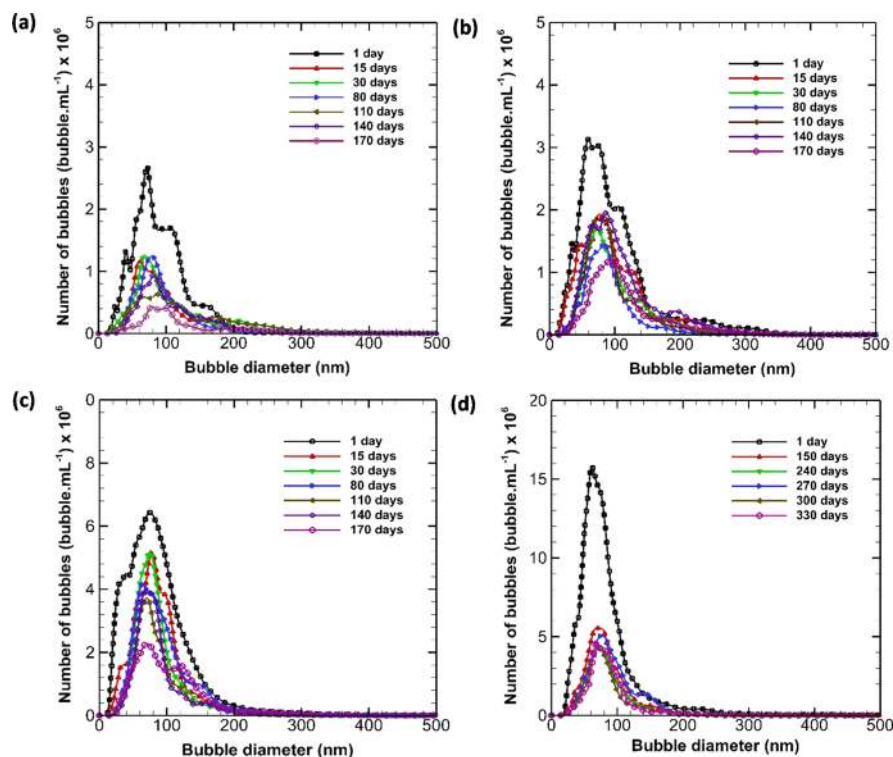
Figure 9. Temporal evolution of the bubble size distribution in nanobubble suspensions of different initial bubble number densities: (a) 2.09×10^8; (b) 2.75×10^8; (c) 5.82×10^8; and (d) 8.89×10^8 bubbles·mL^{-1}.
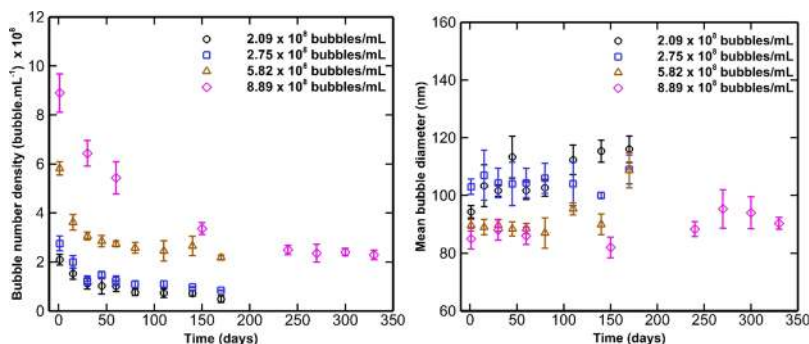
Figure 10. Temporal evolution of bubble number density and mean bubble diameter in nanobubble suspensions of different initial bubble number densities.

alkaline media are more conducive to nanobubble stability than acidic media.

The addition of salt to a nanobubble suspension drives the negative zeta potential toward zero, as depicted in Figure 8b. Again, this phenomenon is well known as "screening of the electric double layer".[43] The value of Debye length (κ^{-1}) can be computed by the following expression

$$\kappa^{-1} = \sqrt{\frac{\varepsilon k_B T}{e^2 I}} \tag{3}$$

where I is the ionic strength of the salt and ε is the medium permittivity. Evidently, the Debye length decreases on addition of salt; for instance, at 1 and 10^3 mM of NaCl, the Debye length is $\kappa^{-1} = 9.61$ and 0.3 nm, respectively. Thus, it is clear from eq 3 that the addition of salt should reduce the repulsive electrostatic forces between nanobubbles.

The addition of the anionic surfactant SDS increases the magnitude of the negative zeta potential, as shown in Figure

8c, because of the adsorption of the sulfate ions (SO_4^-) on the bubble interfaces. A similar behavior has been reported for polystyrene latex particles.[47] Whilst the freeze−thaw experiments discussed above showed that adsorbed surfactant molecules provided a protective layer against the dissolution of nanobubbles, these zeta potential results demonstrate that they also improve their electrostatic stabilization. In conclusion, therefore, the effects of pH, salt, and surfactant addition on the colloidal stability of nanobubbles are similar to those reported for solid nanoparticle suspensions.

Long-Term Stability of Nanobubbles. The most peculiar characteristic of bulk nanobubbles is their extraordinary longevity—they have been reported to last for days and weeks.[1,2,6] Here, we study the long-term stability of nanobubble suspensions by monitoring the evolution of their mean bubble diameter, bubble size distribution, bubble number density, and zeta potential over a period of many months. Four different suspensions with different bubble concentrations

ranging from 2.09×10^8 to 8.89×10^8 bubble·mL^{-1} were generated and preserved in airtight glass vials in a fridge, and samples were withdrawn and analyzed at room temperature at various time intervals. The observation period for the less concentrated suspensions was about 6 months, and for the most concentrated suspension, it approached one year.

The time evolution of the bubble size distributions is presented in Figure 9 for all suspensions. In all cases, the bubble size distribution retains its shape but the peak (i.e., the mode) gradually reduces over time. The bubble number density is plotted in Figure 10 for all samples, showing an exponential decay in the number of nanobubbles, with approximately 50−70% disappearing in the first 50 days. Henceforth, the bubble decay slows down considerably and a significant population is still observed after 170 days in the less concentrated samples and after 330 days in the most concentrated sample. It also seems that the average rate of exponential decay is affected by the initial bubble number density; nanobubbles seem to disappear at a slower rate overall in more concentrated suspensions. Incidentally, on the basis of molecular dynamics simulations, Weijs et al.[1] had reported earlier that diffusive shielding stabilizes bulk nanobubble clusters.

On the whole, there is no significant change in the mean bubble diameter over time except in the case of the least concentrated sample, where the mean diameter witnesses a relatively small but significant increase from about 94 to 118 nm (Figure 10). Because the initial bubble concentration in the sample is the lowest, this modest change in the mean diameter can only be attributed to the increased likelihood of experimental error as the bubble number density approaches the lower resolution limit of the NTA instrument. Thus, it would be reasonable to conclude overall that the mean bubble diameter remains constant over time. Furthermore, the zeta potential (data not shown) also remained unchanged over these periods of sample monitoring.

As the observed nanoentities gradually disappear over time, this implies that they must be nanobubbles. The fact that the mean bubble size remains constant over time suggests the absence of significant effects from bubble coalescence, bubble breakage, or Ostwald ripening. We presume, therefore, that it is the constant surface charge that bulk nanobubbles carry which is probably responsible for their stability. The question then arises as to what is the mechanism behind the observed disappearance of nanobubbles over time. In the case of surface nanobubbles, Ostwald ripening and coalescence have been recently observed by TEM[48] when such bubbles were in close proximity of each other. In the case of bulk nanobubbles, however, as our bubble size and zeta potential measurements suggest, the probability of Ostwald ripening or coalescence must be negligible because of the bubble surface charge. Therefore, there seems to be only three possible mechanisms by which nanobubbles can disappear: (i) nanobubbles could disappear if their surface charge is neutralized, but this was observed to be constant as the zeta potential did not vary; (ii) nanobubbles could perhaps collapse if they come in contact with the hydrophilic surface of the glass storage vial. A more detailed investigation is needed to determine the nature of the interaction of bulk nanobubbles with hydrophobic and hydrophilic surfaces; and (iii) nanobubbles might disappear if they interact with the free surface of the suspension. A very recent study which used cryo-electron microscopy to visualize bulk nanobubbles in aqueous solutions suggested that there were no nanobubbles close to the free surface,[49] which seems to support the possibility that nanobubbles in the upper parts of the suspension may ultimately diffuse to the air−water interface and escape.

Origin of the Nanobubble Surface Charge. Acoustic cavitation involves the generation, expansion, growth, and adiabatic collapse of microscopic cavities or microbubbles. It is known that a high-energy nucleus generated by ultrasonic energy would grow homogeneously in solution, followed by an equilibration between gas in bubble and gas dissolved in water. Microbubbles generated by sonic energy might oscillate with the frequency of sound. At some instant during the sonic compression phase, microbubbles may reduce to a fraction of their size and suddenly collapse. The process of cavity formation and collapse occurs simultaneously at millions of locations, is accompanied by very high local energy dissipation rates, and produces high local temperatures and pressures.[50] This leads to the formation of "hotspots", and highly reactive unstable hydroxyl radicals with a very short lifetime[51,52] are generated. Whilst microbubbles have always been assumed to collapse and vanish, here we presume that the disappearance of such microbubbles gives rise to the formation of nanobubbles which previously went undetected. Cavitation phenomena are complex and difficult to predict, and so it is not inconceivable that nanobubbles may also simultaneously form directly, bypassing the microbubble formation stage. Though the extract origin of the negative surface charge on the nanobubbles cannot be identified with certainty, a possible interpretation can be inferred from the recent literature.[2,53] Ohgaki et al.[2] using infrared spectroscopy measurements, reported the presence of hard hydrogen bonds on bulk nanobubble interfaces. This seems to be consistent with current understanding of the surface charge at an air−water interface, in general, which suggests that water molecules at the interface possess the dangling O−H group pointing out of water at a certain angle, which is responsible for a slight negative charge on the air−water interface. In addition, ions which are loosely bounded in the bulk water can be attracted by the negatively charged interface. Charge transfer causes the surface to reflect the charge on the ions close to the surface, usually anions. Because of such a charge transfer, the water molecules at the surface may become negatively charged, thus, causing the negative charge to increase at the interface.[53,54] This mechanism may be the reason why the observed bulk nanobubbles are negatively charged, as inferred from the zeta potential measurements.

■ CONCLUSIONS

The technique of acoustic cavitation was shown to be effective at producing bulk nanobubbles in pure water in relatively large numbers approaching 10^9 bubble·mL^{-1} with a typical diameter of 100−120 nm. The NTA technique was shown to be more reliable for nanobubble size measurements than DLS which tends to give positively skewed distributions which are biased toward large bubble sizes. Whilst acoustic cavitation is prone to small levels of contamination arising from particles detaching from adjacent solid surfaces, we provided three pieces of evidence which corroborate the hypothesis that the vast majority of the nanoentities generated were nanobubbles: (i) the disappearance of these nanoentities on freezing and thawing of the suspensions; (ii) the strong dependence of their nucleation rate on the amount of dissolved air; and (iii) their gradual disappearance with time.

Long-term monitoring of the nanobubble suspensions over many months showed that the bubble size distribution retains its shape but the peak gradually reduces over time. The bubble number density shows an exponential decay with a significant population of nanobubbles surviving after more than 10 months. There was no significant change in the mean bubble diameter, suggesting the absence of significant bubble coalescence, bubble breakage, or Ostwald ripening effects. The results suggest that bulk nanobubbles carry a negative surface charge, and in pure water, they exhibit a considerable zeta potential of about −24 mV which remains constant over time. Such a constant surface charge is probably the reason behind their stability. The effects of pH, salt, and surfactant addition on the colloidal stability of nanobubbles are similar to those reported in the literature for solid nanoparticle suspensions: (i) an alkaline medium is more conducive to nanobubble stability than an acidic one; (ii) the addition of salt to a nanobubble suspension drives the negative zeta potential toward zero reducing, thus, the repulsive electrostatic forces between nanobubbles; and (iii) the addition of the anionic surfactant SDS increases the magnitude of the negative zeta potential, thus improving their electrostatic stabilization.

■ ASSOCIATED CONTENT

ⓢ Supporting Information

The Supporting Information is available free of charge on the ACS Publications website at DOI: 10.1021/acs.langmuir.8b01163.

Schematics of the NTA and dynamic laser scattering techniques and comparison of nanobubble size distributions obtained by NTA and DLS (PDF)

■ AUTHOR INFORMATION

Corresponding Author

*E-mail: m.barigou@bham.ac.uk.

ORCID ⊙

M. Barigou: 0000-0003-0850-4011

Notes

The authors declare no competing financial interest.

■ ACKNOWLEDGMENTS

■ REFERENCES

(1) Weijs, J. H.; Seddon, J. R. T.; Lohse, D. Diffusive shielding stabilizes bulk nanobubble clusters. *ChemPhysChem* **2012**, *13*, 2197–2204.

(2) Ohgaki, K.; Khanh, N. Q.; Joden, Y.; Tsuji, A.; Nakagawa, T. Physicochemical approach to nanobubble solutions. *Chem. Eng. Sci.* **2010**, *65*, 1296–1300.

(3) Sedlák, M.; Rak, D. Large-scale inhomogeneities in solutions of low molar mass compounds and mixtures of liquids: Supramolecular structures or nanobubbles? *J. Phys. Chem. B* **2013**, *117*, 2495–2504.

(4) Jin, F.; Ye, J.; Hong, L.; Lam, H.; Wu, C. Slow relaxation mode in mixtures of water and organic molecules: Supramolecular structures or nanobubbles? *J. Phys. Chem. B* **2007**, *111*, 2255–2261.

(5) Epstein, P. S.; Plesset, M. S. On the Stability of Gas Bubbles in Liquid-Gas Solutions. *J. Chem. Phys.* **1950**, *18*, 1505–1509.

(6) Ebina, K.; Shi, K.; Hirao, M.; Hashimoto, J.; Kawato, Y.; Kaneshiro, S.; Morimoto, T.; Koizumi, K.; Yoshikawa, H. Oxygen and air nanobubble water solution promote the growth of plants, fishes, and mice. *PLoS One* **2013**, *8*, e65339.

(7) Zimmerman, W. B.; Tesař, V.; Bandulasena, H. C. H. Towards energy efficient nanobubble generation with fluidic oscillation. *Curr. Opin. Colloid Interface Sci.* **2011**, *16*, 350–356.

(8) Ducker, W. A. Contact angle and stability of interfacial nanobubbles. *Langmuir* **2009**, *25*, 8907–8910.

(9) Yasui, K.; Tuziuti, T.; Kanematsu, W.; Kato, K. Dynamic Equilibrium Model for a Bulk Nanobubble and a Microbubble Partly Covered with Hydrophobic Material. *Langmuir* **2016**, *32*, 11101–11110.

(10) Sugano, K.; Miyoshi, Y.; Inazato, S. Study of Ultrafine Bubble Stabilization by Organic Material Adhesion. *Jpn. J. Multiphas. Flow* **2017**, *31*, 299–306.

(11) Agarwal, A.; Ng, W. J.; Liu, Y. Principle and applications of microbubble and nanobubble technology for water treatment. *Chemosphere* **2011**, *84*, 1175–1180.

(12) Ghadimkhani, A.; Zhang, W.; Marhaba, T. Ceramic membrane defouling (cleaning) by air Nano Bubbles. *Chemosphere* **2016**, *146*, 379–384.

(13) Zhu, J.; An, H.; Alheshibri, M.; Liu, L.; Terpstra, P. M. J.; Liu, G.; Craig, V. S. J. Cleaning with bulk nanobubbles. *Langmuir* **2016**, *32*, 11203–11211.

(14) Ushida, A.; Hasegawa, T.; Takahashi, N.; Nakajima, T.; Murao, S.; Narumi, T.; Uchiyama, H. Effect of mixed nanobubble and microbubble liquids on the washing rate of cloth in an alternating flow. *J. Surfactants Deterg.* **2012**, *15*, 695–702.

(15) Calgaroto, S.; Wilberg, K. Q.; Rubio, J. On the nanobubbles interfacial properties and future applications in flotation. *Miner. Eng.* **2014**, *60*, 33–40.

(16) Fan, M.; Tao, D.; Honaker, R.; Luo, Z. Nanobubble generation and its application in froth flotation (part I): Nanobubble generation and its effects on properties of microbubble and millimeter scale bubble solutions. *Min. Sci. Technol.* **2010**, *20*, 1–19.

(17) Fan, M.; Tao, D.; Honaker, R.; Luo, Z. Nanobubble generation and its applications in froth flotation (part II): Fundamental study and theoretical analysis. *Min. Sci. Technol.* **2010**, *20*, 159–177.

(18) Calgaroto, S.; Azevedo, A.; Rubio, J. Separation of amine-insoluble species by flotation with nano and microbubbles. *Miner. Eng.* **2016**, *89*, 24–29.

(19) Sobhy, A.; Tao, D. Nanobubble column flotation of fine coal particles and associated fundamentals. *Int. J. Miner. Process.* **2013**, *124*, 109–116.

(20) Tian, J.; Yang, F.; Cui, H.; Zhou, Y.; Ruan, X.; Gu, N. A novel approach to making the gas-filled liposome real: Based on the interaction of lipid with free nanobubble within the solution. *ACS Appl. Mater. Interfaces* **2015**, *7*, 26579–26584.

(21) Zheng, R.; Yin, T.; Wang, P.; Zheng, R.; Zheng, B.; Cheng, D.; Zhang, X.; Shuai, X.-T. Nanobubbles for enhanced ultrasound imaging of tumors. *Int. J. Nanomed.* **2012**, *7*, 895–904.

(22) Rapoport, N.; Gao, Z.; Kennedy, A. Multifunctional nanoparticles for combining ultrasonic tumor imaging and targeted chemotherapy. *J. Natl. Cancer Inst.* **2007**, *99*, 1095–1106.

(23) Fan, X.; Wang, L.; Guo, Y.; Tu, Z.; Li, L.; Tong, H.; Xu, Y.; Li, R.; Fang, K. Ultrasonic nanobubbles carrying anti-PSMA nanobody: Construction and application in prostate cancer-targeted imaging. *PLoS One* **2015**, *10*, e0127419.

(24) Wang, Y.; Li, X.; Zhou, Y.; Huang, P.; Xu, Y. Preparation of nanobubbles for ultrasound imaging and intracelluar drug delivery. *Int. J. Pharm.* **2010**, *384*, 148–153.

(25) Peyman, S. A.; McLaughlan, J. R.; Abou-Saleh, R. H.; Marston, G.; Johnson, B. R. G.; Freear, S.; Coletta, P. L.; Markham, A. F.; Evans, S. D. On-chip preparation of nanoscale contrast agents towards high-resolution ultrasound imaging. *Lab Chip* **2016**, *16*, 679–687.

(26) Misra, S. K.; Ghoshal, G.; Gartia, M. R.; Wu, Z.; De, A. K.; Ye, M.; Bromfield, C. R.; Williams, E. M.; Singh, K.; Tangella, K. V.; Rund, L.; Schulten, K.; Schook, L. B.; Ray, P. S.; Burdette, E. C.; Pan, D. Trimodal Therapy: Combining hyperthermia with repurposed

bexarotene and ultrasound for treating liver cancer. *ACS Nano* **2015**, *9*, 10695−10718.

(27) Meng, M.; Gao, J.; Wu, C.; Zhou, X.; Zang, X.; Lin, X.; Liu, H.; Wang, C.; Su, H.; Liu, K.; Wang, Y.; Xue, X.; Wu, J. Doxorubicin nanobubble for combining ultrasonography and targeted chemo-therapy of rabbit with VX2 liver tumor. *Tumor Biol.* **2016**, *37*, 8673−8680.

(28) Ushida, A.; Hasegawa, T.; Nakajima, T.; Uchiyama, H.; Narumi, T. Drag reduction effect of nanobubble mixture flows through micro-orifices and capillaries. *Exp. Therm. Fluid Sci.* **2012**, *39*, 54−59.

(29) Kawara, F.; Inoue, J.; Takenaka, M.; Hoshi, N.; Masuda, A.; Nishiumi, S.; Kutsumi, H.; Azuma, T.; Ohdaira, T. The Influences of Pepsin Concentrations and pH Levels on the Disinfective Activity of Ozone Nanobubble Water against Helicobacter pylori. *Digestion* **2014**, *90*, 10−17.

(30) Liu, S.; Oshita, S.; Makino, Y.; Wang, Q.; Kawagoe, Y.; Uchida, T. Oxidative capacity of nanobubbles and its effect on seed germination. *ACS Sustainable Chem. Eng.* **2016**, *4*, 1347−1353.

(31) Liu, S.; Kawagoe, Y.; Makino, Y.; Oshita, S. Effects of nanobubbles on the physicochemical properties of water: The basis for peculiar properties of water containing nanobubbles. *Chem. Eng. Sci.* **2013**, *93*, 250−256.

(32) Matsuki, N.; Ishikawa, T.; Ichiba, S.; Shiba, N.; Ujike, Y.; Yamaguchi, T. Oxygen supersaturated fluid using fine micro/nanobubbles. *Int. J. Nanomed.* **2014**, *9*, 4495−4505.

(33) Oh, S. H.; Yoon, S. H.; Song, H.; Han, J. G.; Kim, J.-M. Effect of hydrogen nanobubble addition on combustion characteristics of gasoline engine. *Int. J. Hydrogen Energy* **2013**, *38*, 14849−14853.

(34) Oh, S. H.; Han, J. G.; Kim, J.-M. Long-term stability of hydrogen nanobubble fuel. *Fuel* **2015**, *158*, 399−404.

(35) Sutherland, W. Dynamical theory of diffusion for non-electrolytes and the molecular mass of albumin. *London, Edinburgh Dublin Philos. Mag. J. Sci.* **1905**, *9*, 781−785.

(36) NanoSight LM10. http://www.malvern.com/en/products/product-range/nanosight-range/nanosight-lm10 (accessed April 7, 2018).

(37) Berne, B. J.; Pecora, R. *Dynamic Light Scattering: With Applications to Chemistry, Biology, and Physics*; Dover Publications, 1976.

(38) Zetasizer Nano ZSP. https://www.malvernpanalytical.com/en/products/product-range/zetasizer-range/zetasizer-nano-range/zetasizer-nano-zsp (accessed April 7, 2018).

(39) Filipe, V.; Hawe, A.; Jiskoot, W. Critical evaluation of nanoparticle tracking analysis (NTA) by NanoSight for the measurement of nanoparticles and protein aggregates. *Pharm. Res.* **2010**, *27*, 796−810.

(40) Oh, S. H.; Kim, J.-M. Generation and stability of bulk nanobubbles. *Langmuir* **2017**, *33*, 3818−3823.

(41) Alheshibri, M.; Craig, V. The puzzling existence of nanobubbles in aqueous solution. *8th Biennial Australian Colloid & Interface*, Coffs Harbour, Australia, Jan 29−Feb 2, 2017.

(42) Duplâtre, G.; Marques, M. F. F.; da Graça Miguel, M. Size of Sodium Dodecyl Sulfate Micelles in Aqueous Solutions as Studied by Positron Annihilation Lifetime Spectroscopy. *J. Phys. Chem.* **1996**, *100*, 16608−16612.

(43) Israelachvili, J. N. *Intermolecular and Surface Forces: With Applications to Colloidal and Biological Systems*; Academic Press, 1985.

(44) German, S. R.; Edwards, M. A.; Chen, Q.; White, H. S. Laplace Pressure of Individual H2 Nanobubbles from Pressure−Addition Electrochemistry. *Nano Lett.* **2016**, *16*, 6691−6694.

(45) Fox, F. E.; Herzfeld, K. F. Gas Bubbles with Organic Skin as Cavitation Nuclei. *J. Acoust. Soc. Am.* **1954**, *26*, 984−989.

(46) Kang, B.-K.; Kim, M.-S.; Park, J.-G. Effect of Dissolved Gases in Water on Acoustic Cavitation and Bubble Growth Rate in 0.83 MHz Megasonic of Interest to Wafer Cleaning. *Ultrason. Sonochem.* **2014**, *21*, 1496−1503.

(47) Brown, W.; Zhao, J. Adsorption of Sodium Dodecyl Sulfate on Polystyrene Latex Particles using Dynamic Light Scattering and Zeta Potential Measurements. *Macromolecules* **1993**, *26*, 2711−2715.

(48) Shin, D.; Park, J. B.; Kim, Y.-J.; Kim, S. J.; Kang, J. H.; Lee, B.; Cho, S.-P.; Hong, B. H.; Novoselov, K. S. Growth Dynamics and Gas Transport Mechanism of Nanobubbles in Graphene Liquid Cells. *Nat. Commun.* **2015**, *6*, 6068.

(49) Li, M.; Tonggu, L.; Zhan, X.; Mega, T. L.; Wang, L. Cryo-EM Visualization of Nanobubbles in Aqueous Solutions. *Langmuir* **2016**, *32*, 11111−11115.

(50) Wu, T. Y.; Guo, N.; Teh, C. Y.; Hay, J. X. W. Theory and Fundamentals of Ultrasound. *Advances in Ultrasound Technology for Environmental Remediation*; Springer: Netherlands, Dordrecht, 2013; pp 5−12.

(51) Attri, P.; Kim, Y. H.; Park, D. H.; Park, J. H.; Hong, Y. J.; Uhm, H. S.; Kim, K.-N.; Fridman, A.; Choi, E. H. Generation mechanism of hydroxyl radical species and its lifetime prediction during the plasma-initiated ultraviolet (UV) photolysis. *Sci. Rep.* **2015**, *5*, 9332.

(52) Elliot, A. J.; McCracken, D. R.; Buxton, G. V.; Wood, N. D. Estimation of rate constants for near-diffusion-controlled reactions in water at high temperatures. *J. Chem. Soc., Faraday Trans.* **1990**, *86*, 1539−1547.

(53) Chaplin, M. Theory versus experiment. What is the charge at the surface of water? *WATER* **2009**, *2*, 1−28.

(54) Chaplin, M. Water Structure and Science. http://www1.lsbu.ac.uk/water/interfacial_water.html (accessed May 26, 2018).